Chinese Journal of Traumatology 23 (2020) 249–257

Contents lists available at ScienceDirect

Chinese Journal of Traumatology

journal homepage: http://www.elsevier.com/locate/CJTEE

Original Article

Global gene expression profiling of blast lung injury of goats exposed to shock wave

Hong Wang [a, b], Wen-Juan Zhang [a], Jun-Hong Gao [b], Jin-Ren Liu [b], Zhi-Yong Liu [a, b], Bao-Qing Xia [b], Xiao-Lin Fan [b], Cun-Zhi Li [b], Ai-Rong Qian [a, *]

[a] Lab for Bone Metabolism, Xi'an Key Laboratory of Special Medicine and Health Engineering, Key Lab for Space Biosciences and Biotechnology, Research Center for Special Medicine and Health Systems Engineering, NPU-UAB Joint Laboratory for Bone Metabolism, School of Life Sciences, Northwestern Polytechnical University, Xi'an 710072, China
[b] Research Center for Toxicological and Biological Effects, Institute for Hygiene of Ordnance Industry, Xi'an 710065, China

ARTICLE INFO

Article history:
Received 7 May 2020
Received in revised form
26 June 2020
Accepted 25 July 2020
Available online 21 August 2020

Keywords:
Blast lung injury
Shock wave
Differentially expressed genes
RNA sequencing
Transcriptome

ABSTRACT

Purpose: Blast lung injury (BLI) is the most common damage resulted from explosion-derived shock wave in military, terrorism and industrial accidents. However, the molecular mechanisms underlying BLI induced by shock wave are still unclear.
Methods: In this study, a goat BLI model was established by a fuel air explosive power. The key genes involved in were identified. The goats of the experimental group were fixed on the edge of the explosion cloud, while the goats of the control group were 3 km far away from the explosive environment. After successful modeling for 24 h, all the goats were sacrificed and the lung tissue was harvested for histopathological observation and RNA sequencing. Gene ontology (GO) and kyoto encyclopedia of genes and genomes (KEGG) analysis were performed to identify the main enriched biological functions of differentially expressed genes (DEGs). Quantitative real-time polymerase chain reaction (qRT-PCR) was used to verify the consistency of gene expression.
Results: Of the sampled goat lungs, 895 genes were identified to be significantly differentially expressed, and they were involved in 52 significantly enriched GO categories. KEGG analysis revealed that DEGs were highly enriched in 26 pathways, such as cytokine-cytokine receptor interaction, antifolate resistance, arachidonic acid metabolism, amoebiasis and bile secretion, JAK-STAT, and IL-17 signaling pathway. Furthermore, 15 key DEGs involved in the biological processes of BLI were confirmed by qRT-PCR, and the results were consistent with RNA sequencing.
Conclusion: Gene expression profiling provide a better understanding of the molecular mechanisms of BLI, which will help to set strategy for treating lung injury and preventing secondary lung injury induced by shock wave.

Introduction

Shock wave-induced lung injury is the most frequent damage resulted from explosions in military, terrorism, industrial accidents, etc.[1,2] It has been estimated that one-tenth of military explosions and six to nine out of ten civilian casualties suffered blast lung injury (BLI) when explosive weapons were used.[3] Clinical reports show that exposure to explosions can cause BLI, resulting in severe clinical manifestations such as acute lung injury (ALI), acute respiratory distress syndrome, and multiple organ dysfunction syndrome, or even death.[4–6] The shock waves produced by explosion firstly reach up to the peak of overpressure in the form of a positive pressure and then decline rapidly to form a negative pressure,[7] which can cause a series of injuries, including the serious damage to lung, gastrointestinal tract, hearing organ, and other gas-containing organs.[5,8] Apnea, bradycardia and hypotension are the three most typical characteristics of lung blast injury.[9] Unfortunately, it is difficult to find the possible causes of lung damage exposed to shock waves and is likely to require novel techniques to elucidate the underlying mechanism.

Previous studies always focus particularly on the BLI damage effects, assessment and treatment, while research on the mechanism of lung injury following exposure to shock waves are

* Corresponding author.
E-mail address: qianair@nwpu.edu.cn (A.-R. Qian).
Peer review under responsibility of Chinese Medical Association.

https://doi.org/10.1016/j.cjtee.2020.08.005

relatively fewer.[10–12] To address the issue, some simulation or small animal models on rat, mouse and rabbit were established to explore the molecular mechanisms of BLI exposed to shock waves. For example, Tong et al.[5] built a mouse model of BLI by a simulation device of explosive knocking, they found that the expression of nuclear factor kappa-B (NF-κB), tumor necrosis factor-α (TNF-α), interleukin-1β (IL-1β), interleukin-6 (IL-6), reactive oxygen species (ROS), melanoma differentiation associated gene 5 (MDA5), Bax and caspase 3 in the lung were increased, indicating that inflammation, oxidative stress and apoptosis may associate with BLI. Chang et al.[13] used a 3D model of computational simulation to investigate the relationships between the distribution of lung surface overpressure and severity of injury. Although a large number of studies have been carried out, the underlying mechanisms of lung injuries induced by blast shock waves is not fully understood.

With the development of high-throughput sequencing technology, RNA sequencing (RNA-seq) has been widely applied to investigate the mechanism of lung injury.[14,15] Identification of shock wave-induced genes from suitable genotypes can provide a springboard to understanding the molecular mechanisms of BLI. Numerous studies have carried out to explore the mechanism of ALI through gene expression analysis. For example, interleukin-18 (IL-18) involved in caspase-1-dependent inflammatory responses,[16] NF-κB-mediated down-regulation of SOX18,[17] TLR4-regulated inflammation and apoptosis by NF-κB and p38 MAPK,[18] TGF-β signaling pathway[19] may play important roles in the regulation of inflammation and apoptosis processes of ALI. However, how these signal pathway proteins were regulated through genes remains unclear; there was no transcriptome analysis to explore the genomic mechanism of BLI till now.

To obtain further insight into the mechanisms of BLI, goats were used to establish BLI models caused by a fuel air explosive in this study. Firstly, the blast-induced lung injury was analyzed with anatomic and pathological methods. Furthermore, RNA-seq analysis was used to explore the differentially expressed genes in lung tissues sampled from blast exposure goats and control group goats. Finally, we applied quantitative real-time polymerase chain reaction (qRT-PCR) technique to verify the RNA-seq results. Our work provides copious resources for the research of the molecular mechanisms of BLI.

Methods

Animals and ethics approval

Six healthy male goats weighing 25−30 kg were purchased from Alxa League of the Inner Mongolia Autonomous region. Animal experiments were conducted according to the guideline of the National Animal Welfare Law of China. The experimental protocols were approved by the ethics committee of the Institute for Hygiene of Ordnance Industry (Xi'an, China). The goats were randomly divided into two groups: experimental group and control group with 3 goats in each.

Goats exposed to shock waves

The BLI model was completed by a fuel air explosive power. As shown in Fig. 1A, the fuel air explosive was implemented on the top of a bracket 3 m above the ground. The goats of the experimental group and shock wave sensor were fixed on the arc of 35 m from the explosive center where the edge of the explosion clouds was. The shock wave data were obtained by the pressure sensor, then they were transmitted and stored in a computer. The shock wave sensor was placed in a special fixator which located on the same level of the ground. Fig. 1B showed the fixed approach of goats. In detail, each of the goats in the experimental group and the control group was wearing a special vest that was fixed on the supporting structure embedded in the ground to avoid movement. In the experimental group, the right side of the goat body faced the explosive center. By contrast, the goats of the control group were fixed 3 km away from the explosive center. The relationship between the peak of overpressure and distance is shown in Fig. 1C.

Sample preparation and hematoxylin-eosin (HE) staining

After successful modelling for 24 h, all the goats were fixed on an operating table and sacrificed by bloodletting through the cervical artery. After open the thoracic cavity, the lung was obtained. To ensure the consistency and validation of the samples, lung tissue blocks of the same size and same location in the middle lobe of the right lung were taken and stored in liquid nitrogen for RNA-seq analysis. And another piece of lung tissue in the middle lobe was fixed in 10% (v/v) formaldehyde for one week at room temperature and dehydrated using the Fully Enclosed Tissue Processor (ASP300S, Leica Biosystems, Germany) before embedding in paraffin (EG1150H + C, Leica Biosystems, Germany). The fixed paraffin lung tissues were cut into 5 μm-thick sections using the microtome (RM2245, Leica Biosystems, Germany) and then stained with H&E Staining System (ST5020, Leica Biosystems, Germany) according to the instructions. The sections were visualized with a light microscope (DM4000B, Leica Microsystems, Germany).

RNA sequencing

The total RNA extraction and quality control were extracted according to the protocols available in the literature.[20] RNA library construction and sequencing were conducted by Annoroad Gene Technology Co., Ltd. (Beijing, China). Detailed methods were described as references.[21,22] Briefly, libraries were generated using Illumina mRNA Library Prep Kit (#E7530L, NEB, USA). The concentration and insert size of libraries were measured by using Real-Time PCR Detection system (CFX 96 Touch, Bio-RAD, USA) and Agilent Bioanalyzer 2100 system (Agilent Technologies, CA, USA), respectively. Qualified libraries were sequenced on an Illumina HiSeq Xten Sequencer and 150 bp paired-end reads were generated.

Data analysis

After removing the reads with low-quality and high poly-N, the clean reads were mapped to the goat reference genome using HISAT2 software (Vison 2.1.0). Then, fragments per kilobase million mapped reads were calculated to estimate the expression level of each gene. The R package DESeq2 was used to identify DEGs with a threshold of $q \leq 0.05$ and $|\log_2 \text{fold change}| \geq 1$. Gene ontology (GO) and kyoto encyclopedia of genes and genomes (KEGG) pathways analysis were performed to identify the main enriched biological functions of the DEGs. The $q < 0.05$ was considered to be significant expressed genes.

qRT-PCR

Fifteen DEGs that enriched in the pathways were selected for qRT-PCR to evaluate the expression data 18S from RNA-seq. Primer sequences were showed in Appendix 1. First-strand cDNA was synthesized using the PrimerScript™ RT Reagent Kit with cDNA Eraser (TaKaRa, Dalian, China). qRT-PCR was performed on each sample in triplicate using SYBR® Premix Ex Taq (TaKaRa, Dalian, China) on 7500 Fast Real-Time PCR system (Applied Biosystems). The polymerase chain reaction (PCR)

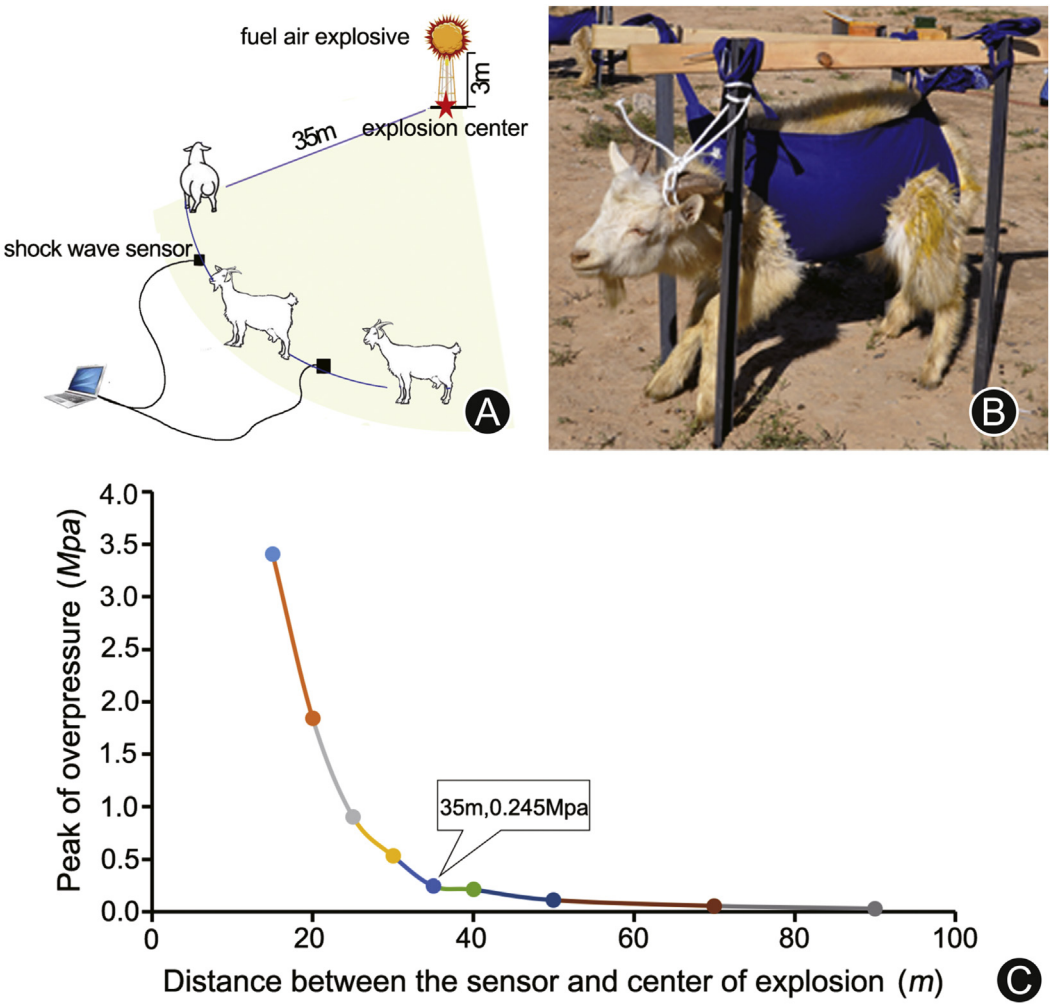

Fig. 1. (A) The explosion field (the radius of the shock wave was 90 m, the height of fuel air explosive was 3 m, the distance between the explosion center and the goat was 35 m); (B) the fixed approach of goats; (C) the relationship between the peak of overpressure and distance. The peak of overpressure was 0.245 MPa at the point of 35 m, where the test goats were placed.

amplification procedure was as follows: initial denaturation at 95°C for 30 s, followed by 40 cycles at 95°C for 5 s and 60°C for 30 s. Melting curve analysis was used to check amplification specificity. Expression analysis was performed with reference to the 18s actin gene. The $2^{-\Delta CT}$ method was used to analyze the relative changes in transcript expression.[23] Statistical analysis was performed using SPSS software (version 23.0, authorization code: ed5a8d700■197e09c3a).

Results

Anatomy and histopathology analysis of the goat lung exposed to shock waves

As shown in Fig. 2, the gross anatomy results indicated that obvious bullae, congestion and bleeding were observed in the goat lungs of the experimental group, compared with the control group. In addition, there were significant hyperemia and edema of bronchial mucosa as well as exfoliated epithelial cells in the goat lungs of the experimental group under microscope. Notably, reddish edema fluid, erythrocyte, and even focal or patchy bleeding occurred in the alveolar cavity. These results suggested that there was serious lung injury of the goats exposed to the shock wave.

Alignment and assembly of RNA-Seq data

Six cDNA libraries of goat samples in the control group (C1, C2, C3) and the experimental group exposed to shock waves (T1, T2, T3) were sequenced, and about 3 GB of data of each sample were generated. The overall quality of the six libraries was shown in Table 1. After trimming the low-quality sequences, 139, 157, 178 reads and 134, 260, 730 reads were obtained for all samples of the experimental group and the control group, respectively. And the Q30 (the percentage of bases with a phred value > 30) of each sample was more than 93%. The clean data were obtained by comparison to the reference genome using HISAT2 software (version 2.1.0), the mapped read numbers for the experimental group and the control group are 134, 943, 759 and 130, 101, 053, respectively. The rates of all samples were more than 96%.

Fragments per kilobase of transcript per million fragments mapped (FPKM), which can be used to describe the characteristics of gene expression. In six samples, 65.41%–65.76% of the mRNA transcripts were detected as FPKM > 1, and 4.68%–5.29% was detected as FPKM > 60. The accuracy and reliability of gene expression were assessed by Pearson's correlation coefficients (R^2). The R^2 values were larger than 0.99 between three samples of each group, which revealed a good performance of libraries in the lung of goats (Appendix 2).

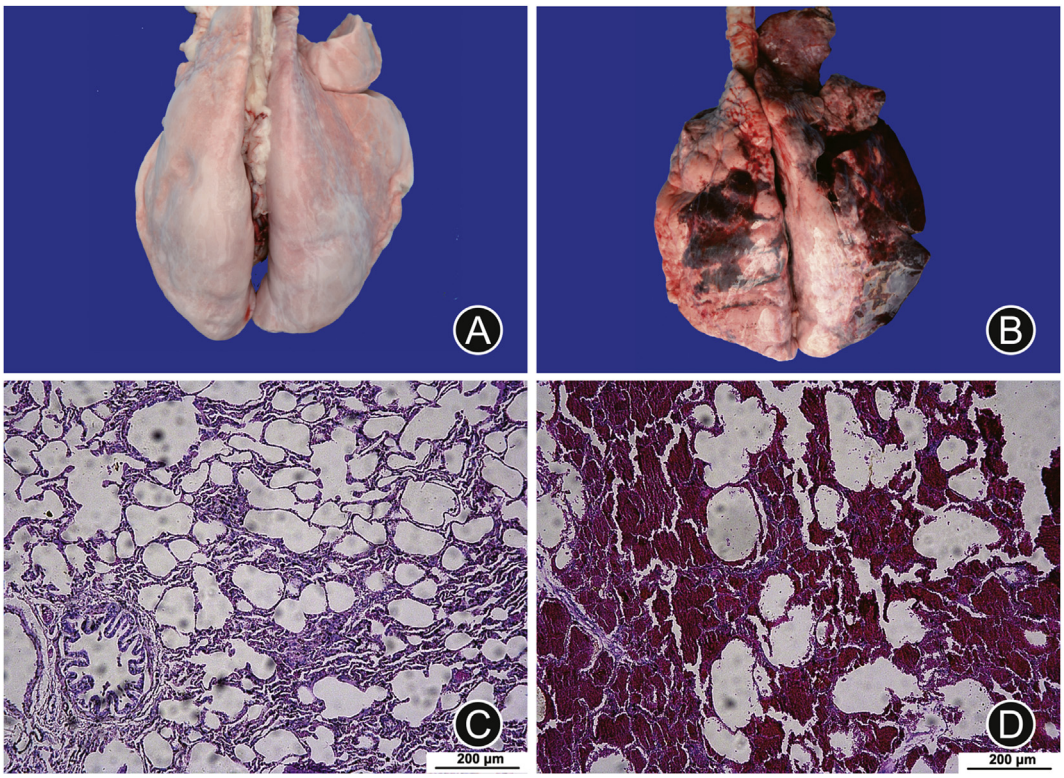

Fig. 2. Comparison of anatomy and histopathology between the control group and the experimental group. (A) and (B) were normal lung of the control group and injured lung exposed to shock wave, respectively. (C) and (D) were microscopic observation of lung tissue for the control group and the experimental group induced by shock wave, respectively. Hematoxylin-eosin staining, ×10 amplification, scale bar: 200 μm.

Table 1
The quality of RNA-Seq data.

Sample	C1[a]	C2[a]	C3[a]	T1[b]	T2[b]	T3[b]
Raw reads, *n*	45,397,848	49,030,928	46,502,552	47,276,996	48,213,416	49,043,910
Clean reads, *n*	42,956,812	46,805,200	44,444,718	45,851,248	46,560,438	46,745,492
Clean bases, *n*	6,443,521,800	7,020,780,000	6,666,707,700	6,877,687,200	6,984,065,700	7,011,823,800
Q30 (%)	93.92	94.06	93.83	93.91	94.08	94.12
Total-mapped, *n* (%)	41,654,953 (96.97)	45,403,546 (97.01)	43,042,554 (96.85)	44,465,804 (96.98)	45,142,364 (96.95)	45,335,591 (96.98)
Uniquely-mapped, *n* (%)	40,113,769 (96.30)	43728,229 (96.31)	41,463,802 (96.33)	42,827,550 (96.32)	43,460,062 (96.27)	43,573,934 (96.11)

C1, C2 and C3 represented the sample numbers of the control group, while T1, T2 and T3 represented the sample numbers of the experimental group.
[a, b] indicated libraries derived from the lung of goat in three biological replicates for the control and the experimental group, respectively.

Table 2
Gene symbol and name.

Gene symbol	Gene name
FASLG	Fas ligand
IL10	Interleukin-10
SOCS3	Suppressor of cytokine signaling 3
OSMR	Oncostatin-*M*-specific receptor
CDKN1A	Cyclin-dependent kinase inhibitor 1
CSF3R	Granulocyte colony-stimulating factor receptor
IL6	Interleukin-6
CXCL8	C-X-C motif chemokine ligand 8 (IL8)
COL1A1	Collagen Type I Alpha 1
COL3A1	Collagen Type III Alpha 1
COL1A2	Collagen Type I Alpha 2
CD14	Lipopolysaccharide receptor
LOC102182395	Growth-regulated alpha protein
LOC102188986	HLA class II histocompatibility antigen
LOC102176878	Mast cell protease 3

Identification of DEGs of goat lungs exposed to shock wave

After evaluating the quality of the sequencing data, the DEGs were identified with a threshold of $q < 0.05$ and $|\log_2 FC| > 1$. A total of 21,916 DEGs were identified, which were clustered into two groups by hierarchical clustering according to their expression patterns (Fig. 3). Among the DEGs, 895 genes were identified as significantly differentially expressed between the control and the experimental group ($p < 0.05$), including 516 up-regulated and 379 down-regulated genes. Furthermore, 65 genes ($|\log_2 FC| > 4$) were highly expressed in goat lungs exposed to shock wave, such as LOC102170003 (8.0-$\log_2$FC), PRG4 (7.8-$\log_2$FC), LOC102175876 (7.1-$\log_2$FC), ANKRD1 (6.7-$\log_2$FC), IL1R2 (4.5-$\log_2$FC), LOC108634205 (−8.0-$\log_2$FC), LOC102171242 (−7.4-$\log_2$FC). In addition, 196 genes ($2 < |\log_2$ fold change$| < 4$) were mildly expressed, including several protein families, such as FOSL1 (3.9-$\log_2$FC), PAPPA2 (3.7-$\log_2$FC), LOC102168428 (2.3-$\log_2$FC), IL6 (2.0-$\log_2$FC), IL1RL2 (−3.9-$\log_2$FC), LOC108637258 (−3.6-$\log_2$FC), IL5RA (−2.0-$\log_2$FC). The details of the DEGs were shown in Appendix 3.

GO and KEGG pathway analysis

GO enrichment analysis indicated that DEGs were enriched into 52 GO categories ($q < 0.05$), which were involved in 17 “cellular components”, 23 “biological process” and 12 “molecular function”.

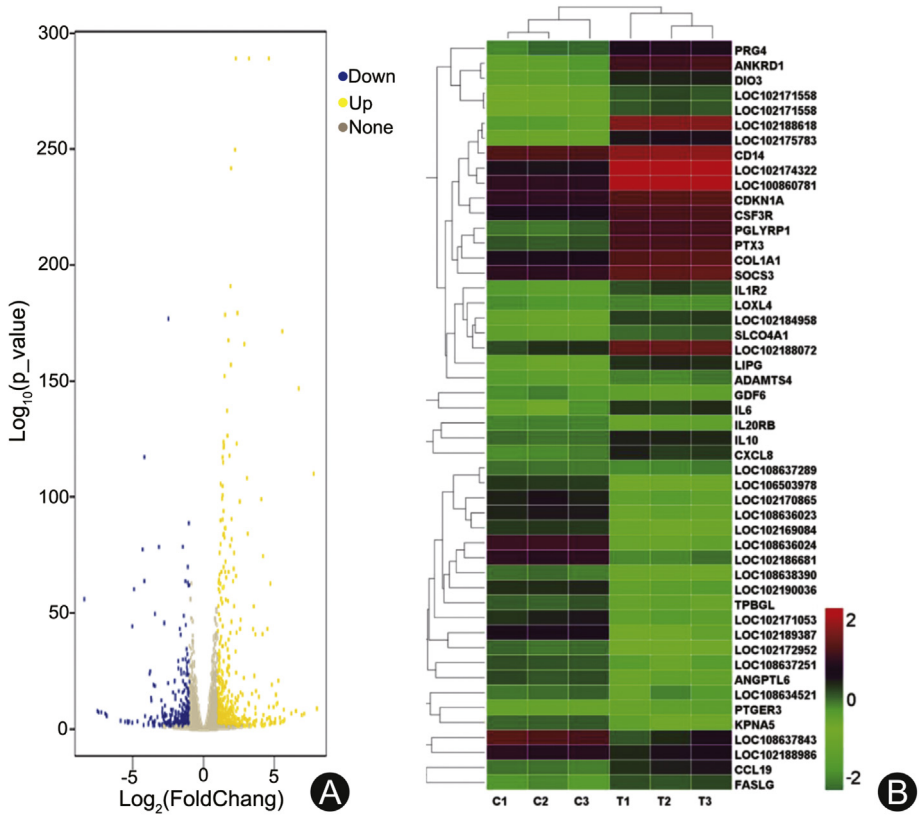

Fig. 3. (A) Volcano plot of DEGs in the test and the control group. Yellow points represent the up-regulated genes with $|\log_2 \text{fold change}| > 1$ and adjusted $q < 0.05$. Blue points represent down-regulated genes with $|\log_2 \text{fold change}| < -1$ and $q < 0.05$. Grey points represent genes with no significant difference. (B) The heatmap showing the expression levels of top 50 DEGs which we are more interested in. The color bar represents the level of expression of DEGs. DEGs: differentially expressed genes.

The 17 enriched sub-categories of "molecular components" included extracellular region, cell, membrane, virion, cell junction, membrane-enclosed lumen and so on. The 23 enriched sub-categories belonging to "biological process", such as cell killing, immune system process, behavior, metabolic process, cell proliferation, cellular process, reproductive process, are closely associated with apoptosis, immune response and inflammation.[5,24] The 12 enriched sub-categories of "molecular function" were involved in catalytic activity, signal transducer activity, structural molecule activity, transporter activity, binding, antioxidant activity, protein tag, molecular transducer activity and so forth. The GO analysis results indicated that DEGs were more likely to be involved in apoptosis, immune response, inflammation and oxidative stress (Fig. 4 and Appendix 4).

To further clarify the molecular and biological functions, the DEGs were mapped into the KEGG database. KEGG pathway analysis demonstrated that they were involved in 256 pathways, of which 26 pathways were significantly enriched ($q < 0.05$). The top five significantly enriched pathways of DEGs were associated with cytokine-cytokine receptor interaction, antifolate resistance, arachidonic acid metabolism, amoebiasis and bile secretion signaling pathway. Among them, cytokine-cytokine receptor interaction pathway was related to the largest number of 28 DEGs. Besides, they also include some inflammatory responses related pathways such as JAK-STAT and IL-17. (Fig. 5 and Appendix 5). Therefore, these three pathways were selected for further analysis.

The validation of DEG expression by qRT-PCR

To verify the gene expression of RNA-seq analysis, 15 DEGs involved in cytokine-cytokine receptor interaction, amoebiasis, JAK-STAT signaling pathway and IL-17 signaling pathway were selected and validated by qRT-PCR. Among them, 13 genes were up-regulated (FASLG, IL-10, IL-6, SOCS3, OSMR, CDKN1A, CSF3R, CXCL8, COL1A1, COL3A1, COL1A2, CD14, LOC102182395) and 2 genes were down-regulated (LOC102188986 and LOC102176878). The qRT-PCR results showed that it is very consistent with RNA-seq data (Fig. 6).

Discussion

In this study, the BLI model of goat was successfully established by a fuel air explosive. The advantage of this work is that the model is achieved with large animals in live-fire explosive conditions. Goats were selected for modelling in our study. The lung of goats with body weight 20–25 kg is similarly to that of adults, which is essential to dynamically investigate the structure and function changes induced by an explosion.[25] A report from the US Army Medical Research and Materiel Command revealed that they established a log-logistic model of dose-response curves and lethality correlation with 1200 sheep exposed to air blast in free-field and confined enclosures, which can be used for predicting the survivability of BLI thus understanding the underlying mechanisms.[26] In addition, compared with large animals, small animals (such as murine and rat) are widely used in blast injury studies, because they are easier to handle and perform molecular mechanism exploration. For instance, Mikulas et al.[27] established a blast overpressure rat lung injury model and they revealed that the oxidant stress and inflammation play important roles in BLI. Hafner et al.[28] found chest trauma induced by blast shock wave significantly increased parameters of local inflammation, purinergic receptor expression and nitrotyrosine formation. In summary, small and large animals are very different in terms of body shape, organ

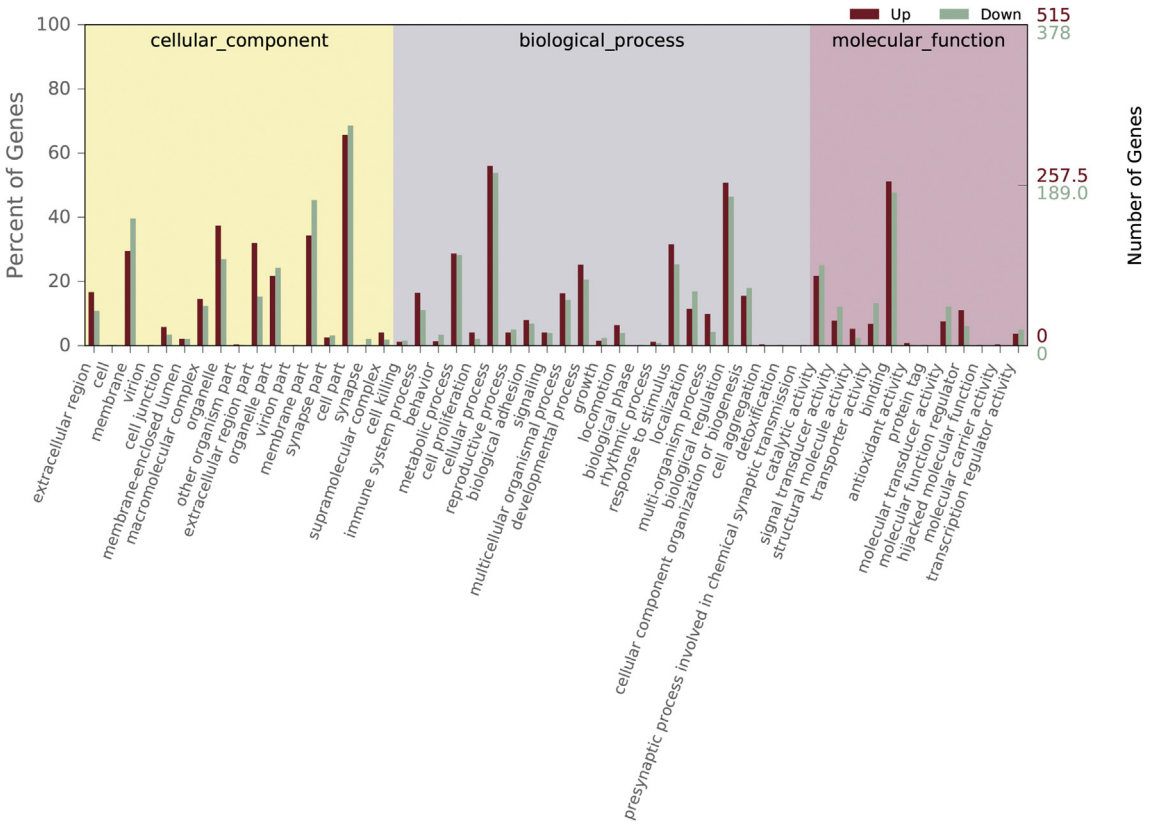

Fig. 4. Gene ontology annotation and classification of differentially expressed genes between the control and the experimental group.

size, metabolic rate, breathing rate, and many other parameters. In fact, rodents are more vulnerable to be suffered from BLI under blast shock wave because of lower normalized lung density.[29] Notably, the structure, physiological function and injury responses in the lung of large animals are more similarly to that of human. Therefore, large animals (such as goat) are more valuable to explore the mechanisms of BLI, which may provide the guidance for the clinical treatment of BLI in human.

It was reported that lung injuries were considered as severe (31%–60% of ecchymosis) when the incident impulse exceed 0.233 MPa.[10] In our study the peak value of shock wave was 0.245 MPa where the goats of experimental group were exposed. In line with the literature, the results of anatomy and histopathology proved that the model was successfully established. And yet, the biological characteristics of fuel air explosive power were obtained, which could not only provide reliable technical support for the biological damage assessment, but also offer a theoretical basis for the treatment and protection of BLI. The study aimed to investigate the physiological and molecular biological changes in the acute stage (within 24 h) of BLI, which may provide guidance for the diagnosis of blast injury. Acute effects were generally occurred in the lungs of goats induced by blast waves, including the changes in the respiratory and circulatory systems, pulmonary hemorrhage, and hypoxemia caused by pulmonary edema. A large number of neutrophils and alveolar macrophages were aggregated and activated in the lung, leading to the secretion of inflammatory cytokines or oxygen radical.[30] Therefore the inflammation and oxidative stress were stimulated in the time window within 24 h after injury, which was considered to be very important for the diagnose of BLI.

So far, transcriptome analysis is one of the mainstream methods to illustrate the molecular mechanisms of lung injury induced by physical or chemical.[31,32] However, there have been no reports of lung injury caused by blast or shock wave using transcriptomic sequencing at present. In the study, 895 genes were identified to be differentially expressed between blast exposure group and control goats. GO and KEGG pathway analyses revealed that the DEGs were highly enriched in as many as 26 signaling pathways as previous describing, which can provide direction for mechanism research. Among these pathways, cytokine-cytokine receptor interaction, IL-17 and JAK-STAT were involved in inflammatory response. Numerous studies revealed that blast could cause inflammation in lung tissue, then impairing the structure and physiological functions of lung occurred immediately.[33,34] These three pathways mentioned above would provide novel perspective for the dissection of the mechanisms of inflammatory response in blast injury lungs. Our previous study found that fibrous tissue hyperplasia is the other characteristic of lung tissue damaged by explosion, which may be associated with the activation of the amoebiasis pathway.

Moreover, 15 key genes involved in those pathways were selected and validated by qRT-PCR. The verified results were consistent with the RNA sequencing results. In agreement with literature reports, SOCS3,[35,36] OSM,[37,38] IL-6,[5,36] IL-10,[39] CXCL-1[5] and CXCL-8[17] increased significantly, so inflammatory factors-mediated injury is an important factor of BLI. OSMR and CDNK1A are the genes related to inflammatory response, cell growth and proliferation and involved in the JAK-STAT3 signaling pathway.[38] In accordance with references[40–42], we also found that the expressions of FASLG and CD14 increased significantly, suggesting that it may be involved in the immune response in BLI. This may provide a new tool to find useful targets for monitoring, evaluating, even weakening the overwhelming inflammatory response of patients with blast injury. Type I collagen and type III collagen, the important members of the collagen family are the key structural

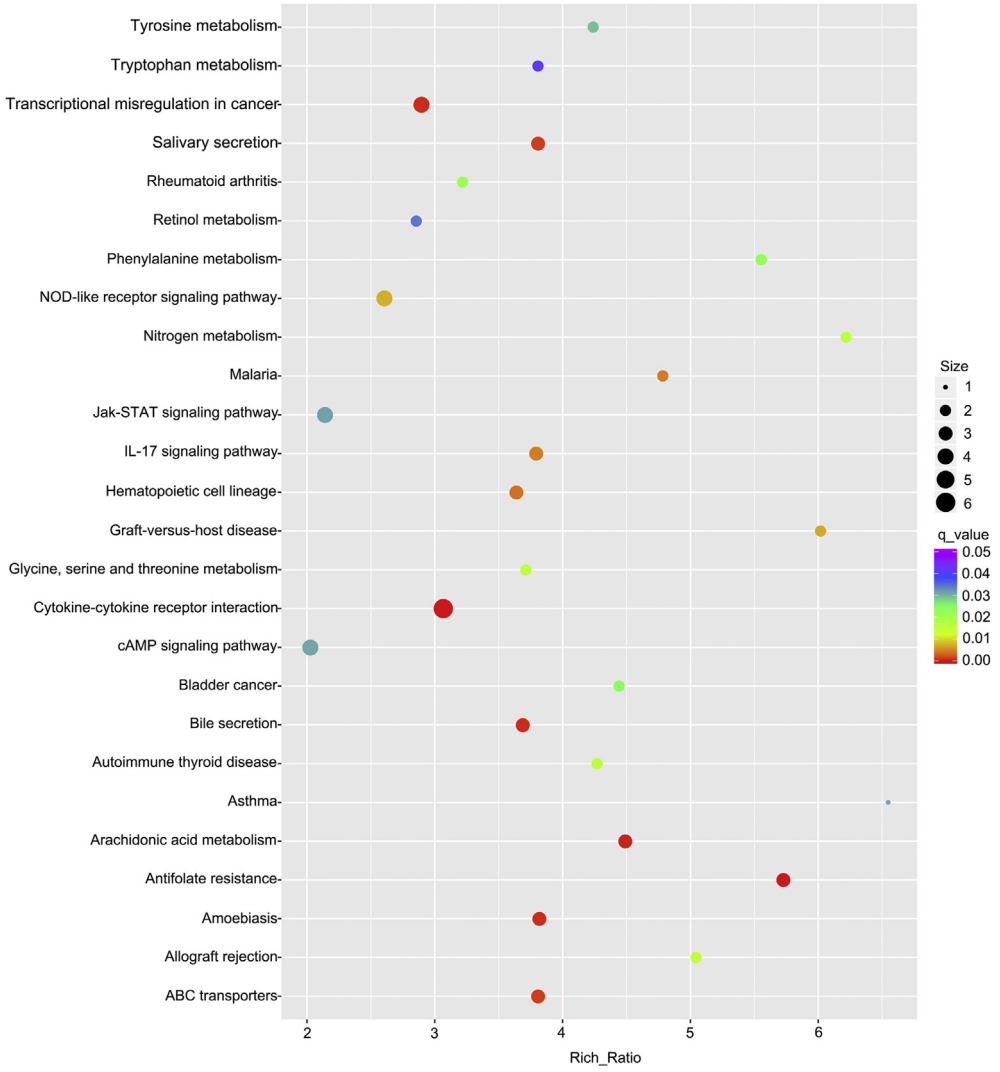

Fig. 5. Significantly enriched KEGG pathways of differentially expressed genes between the control and the experimental group. The horizontal and vertical coordinates represent rich ratio and KEGG pathway name. The size of black dots and the color strip represent the gene number and range of the *q*, respectively. KEGG: kyoto encyclopedia of genes and genomes.

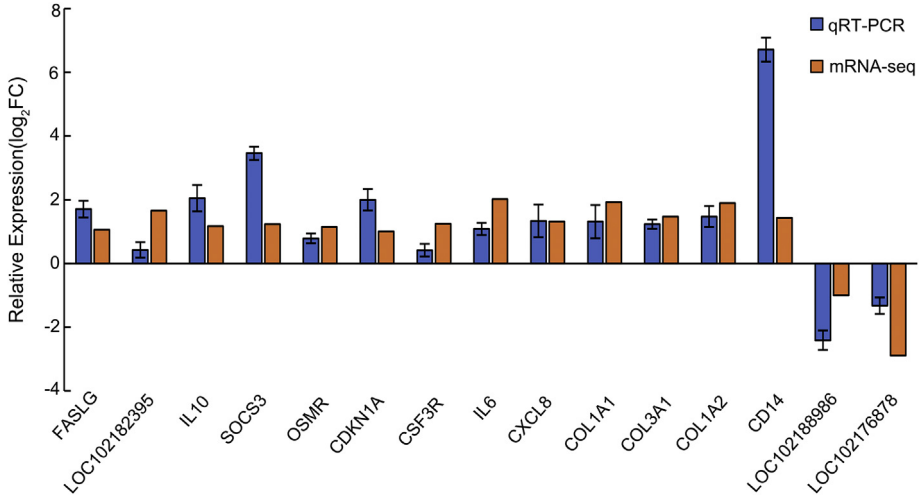

Fig. 6. Verification of gene expression between RNA-seq and qRT-PCR. The horizontal and vertical coordinates represent genes name and the relative expression values which were normalized using 18s RNA gene. The standard deviation is shown by the error bar. Relative expression $\log_2$FC refers to the logarithmic value (base 2) for the fold change of differentially expressed genes between the test and control group. The gene symbols and names are shown in Table 2.

components of the extracellular matrix[43] and hollow organs such as vessels.[44,45] In our study, the expression of COL1A1, COL1A2 and COL3A1 genes were significantly increased, indicating that collagen family was also involved in the process of BLI. The expression of LOC102188986 and LOC102176878 genes were significantly down-regulated, which refers to HLA class II histocompatibility antigen[46] and mast cell protease 3 involving the inflammatory response of BLI.[47,48]

In summary, a BLI model of goat was successfully established by a fuel air explosive in this study. Total of 895 DEGs were identified by RNA-seq analysis, with 516 up-regulated and 379 down-regulated genes. Fifty-two GO categories and 26 pathways related to BLI were analyzed, such as inflammatory and immune response-related pathways. Moreover, 15 key genes were validated by qRT-PCR, of which the results were excellent agreement with the RNA-seq data. This study provided a research strategy to dissect potential mechanisms of BLI. The data we presented are primary, more complex mechanistic studies based on a great deal of experimental evidences are necessary. In addition, more accurate targets are waiting to be clarified, which might be helpful to explore the detail molecular regulation mechanism, to find some suitable ways for the early diagnosis and treatment of BLI, even look for a strategy to predict the prognosis of BLI.

Funding

This work was supported by Science and Technology Development Fund for Institute for Hygiene of Ordnance (KY202007).

Ethical Statement

The experimental protocols were approved by the Ethics Committee of the Institute for Hygiene of Ordnance Industry (Xi'an, China).

Acknowledgments

The authors would like to thank the Institute for Hygiene of Ordnance Industry and the School of Life Sciences at Northwestern Polytechnical University for continued support.

Declaration of Competing Interest

The authors declare no conflict interests.

Appendix A. Supplementary data

Supplementary data to this article can be found online at https://doi.org/10.1016/j.cjtee.2020.08.005.

References

1. Magnusa D, Mansoor AK, William GP. Epidemiology of civilian blast injuries inflicted by terrorist bombings from 1970-2016. *Defence Technology*. 2018;14:469–476. https://doi.org/10.1016/j.dt.2018.07.014.
2. Scott TE, Kirkman E, Haque M, et al. Primary blast lung injury - a review. *Br J Anaesth*. 2017;118:311–316. https://doi.org/10.1093/bja/aew385.
3. Sziklavari Z, Molnar TF. Blast injures to the thorax. *J Thorac Dis*. 2019;11:167–171. https://doi.org/10.21037/jtd.2018.11.106.
4. Mackenzie IM, Tunnicliffe B. Blast injuries to the lung: epidemiology and management. *Phil Trans R Soc B*. 2011;366:295–299. https://doi.org/10.1098/rstb.2010.0252.
5. Tong CC, Liu YE, Zhang YB, et al. Shock waves increase pulmonary vascular leakage, inflammation, oxidative stress, and apoptosis in a mouse model. *Exp Biol Med*. 2018:1–11. https://doi.org/10.1177/1535370218784539, 0.
6. Alastair B, Paul P. Blast injuries: a guide for the civilian surgeon. *Surgery*. 2018;36:394–401. https://doi:10.1016/j.mpsur.2018.05.007.
7. Van der Voort MM, Holm KB, Kummer PO, et al. A new standard for predicting lung injury inflicted by Friedlander blast waves. *J Loss Prevent Proc*. 2016;40:396–405. https://doi:10.1016/j.jlp.2016.01.014.
8. Logan NJ, Arora H, Higgins CA. Evaluating primary blast effects in vitro. *JoVE*. 2017;127, e55618. https://doi:10.3791/55618.
9. CDC offers primer on blast injury care. *J Am Med Assoc*. 2013;309:2088. https://doi:10.1001/jama.2013.5628.
10. Boutillier J, Deck C, De Mezzo S, et al. Lung injury risk assessment during blast exposure. *J Biomech*. 2019;86:210–217. https://doi:10.1016/j.jbiomech.
11. Westrol MS, Donovan CM, Kapitanyan R. Blast physics and pathophysiology of explosive injuries. *Ann Emerg Med*. 2017;6:S4–S9. https://doi:10.1016/j.annemergmed.2016.09.005.
12. Chang Y, Zhang DH, Hu Q, et al. Usage of density analysis based on micro-CT for studying lung injury associated with burn-blast combined injury. *Burns*. 2018;44:905–916. https://doi:10.1016/j.burns.2017.12.010.
13. Chang Y, Zhang DH, Liu LY, et al. Simulation of blast lung injury induced by shock waves of five distances based on finite element modeling of a three-dimensional rat. *Sci Rep*. 2019;9:3440. https://doi:10.1038/s41598-019-40176-7.
14. dos Santos CC, Okutani D, Hu P, et al. Differential gene profiling in acute lung injury identifies injury-specific gene expression. *Crit Care Med*. 2008;36:855–865. https://doi:10.1097/CCM.0B013E3181659333.
15. Rajasekaran S, Pattarayan D, Rajaguru P, et al. MicroRNA regulation of acute lung injury and acute respiratory distress syndrome. *J Cell Physiol*. 2016;231:2097–2106. https://doi:10.1002/jcp.25316.
16. Dolinay T, Kim YS, Howrylak J, et al. Inflammasome-regulated cytokines are critical mediators of acute lung injury. *Am J Respir Crit Care Med*. 2012;185:1225–1234. https://doi:10.1164/rccm.201201-0003OC.
17. Zhou Y, Hao C, Li C, et al. mentin-1 protects against bleomycin-induced acute lung injury. *Mol Immunol*. 2018;103:96–105. https://doi:10.1016/j.molimm.2018.09.007.
18. Li H, Shi H, Ma N, et al. BML-111 alleviates acute lung injury through regulating the expression of lncRNA MALAT1. *Arch Biochem Biophys*. 2018;649:15–21. https://doi:10.1016/j.abb.2018.04.016.
19. Riemondy KA, Jansing NL, Jiang P, et al. Single-cell RNA sequencing identifies TGF-β as a key regenerative cue following LPS-induced lung injury. *JCI Insight*; 2019:123637. https://doi:10.1172/jci.insight.123637.
20. Brown RAM, Epis MR, Horsham JL, et al. Total RNA extraction from tissues for microrna and target gene expression analysis: not all kits are created equal. *BMC Biotechnol*. 2018;18:16. https://doi:10.1186/s12896-018-0421-6.
21. Bai S, Liu W, Wang H, et al. Enhanced herbicide metabolism and metabolic resistance genes identified in tribenuron-methyl resistant myosoton aquaticum L. *J Agric Food Chem*. 2018;66:9850–9857. https://doi:10.1021/acs.jafc.8b02740.
22. Hu Y, He C, Liu JP, et al. Analysis of key genes and signaling pathways involved in Helicobacter pylori-ssociated gastric cancer based on the Cancer Genome Atlas database and RNA sequencing data. *Helicobacter*. 2018;23, e12530. https://doi.org/10.1111/hel.12530.
23. Livak KJ, Schmittgen TD. Analysis of relative gene expression data using real-time quantitative PCR and the 2−ΔΔCT method. *Methods*. 2001;25:402–408. https://doi:10.1006/meth.2001.1262.
24. Chen KH, Yang J, Xiao F, et al. Early peritoneal dialysis ameliorates blast lung injury by alleviating pulmonary edema and inflammation. *Shock*; 2019. https://doi:10.1097/SHK.0000000000001325.
25. Scheerlinck J-PY. The immune system of sheep and goats. *Encyclopedia of Immunobiology*; 2016:526–531. https://doi:10.1016/B978-0-12-374279-7.12017-X.
26. MacFadden LN, Chan P, Ho KH, et al. A model for predicting primary blast lung injury. *J. Trauma Acute Care Surg*. 2012;73:1121–1129. https://doi:10.1097/TA.0b013e31825c1536.
27. Chavko M, Prusaczyk WK, McCarron RM. Lung injury and recovery after exposure to blast overpressure. *J Trauma*. 2006;61:933–942. https://doi.org/10.1097/01.ta.0000233742.75450.47.
28. Hafner S, Wagner K, Wepler M, et al. Physiological and immune-biological characterization of a long-term murine model of blunt chest trauma. *Shock*. 2015;43:425. https://doi.org/10.1097/shk.0000000000000277. Shock. 2015;43(2):140-147.
29. Wood GW, Panzer MB, Courtney AC, et al. Interspecies scaling in blast pulmonary trauma. *HMDS*. 2018;2:3. https://doi:10.1007/s41314-018-0013-1.
30. Zhou X, Dai Q, Huang X. Neutrophils in acute lung injury. *Front Biosci*. 2012;17:2278–2283. https://doi.org/10.2741/4051.
31. Hrdlickova R, Toloue M, Tian B. RNA-Seq methods for transcriptome analysis: RNA-Seq. *Wiley Interdiscip Rev RNA*. 2017;8:e1364. https://doi:10.1002/wrna.1364.

32. Huang JQ, Li YJ, Liu Z, et al. Transcriptomic responses to heat stress in rainbow trout Oncorhynchus mykiss head kidney. *Fish Shellfish Immunol*. 2018;82: 32–40. https://doi:10.1016/j.fsi.2018.08.002.
33. Cho HJ, Sajja VS, Vandevord PJ, et al. Blast induces oxidative stress, inflammation, neuronal loss and subsequent short-term memory impairment in rats. *Neuroscience*. 2013;253:9–20. https://doi.org/10.1016/j.neuroscience.2013.08.037.
34. Gill J, Motamedi V, Osier N, et al. Moderate blast exposure results in increased IL-6 and TNFα in peripheral blood. *Brain Behav Immun*. 2017;65:90–94. https://doi.org/10.1016/j.bbi.2017.02.015.
35. Croker BA, Krebs DL, Zhang JG, et al. SOCS3 negatively regulates IL-6 signaling in vivo. *Nat Immunol*. 2003;4:540–545. https://doi:10.1038/ni931.
36. Reda E, Hassaneen S, El-Abhar HS. Novel trajectories of bromocriptine antidiabetic action: leptin-IL-6/JAK2/p-STAT3/SOCS3, p-IR/p-AKT/GLUT4, PPAR-γ/adiponectin, nrf2/PARP-1, and GLP-1. *Front Pharmacol*. 2018;9:771. https://doi:10.3389/fphar.2018.00771.
37. Nevin K, Stawski L, Feeney M, et al. THU0026 Osm is more effective than il-6 at inducing endomt of human dermal microvascular cells. *Ann Rheum Dis*. 2017;76, 209.1-209 https://doi:10.1136/annrheumdis-2017-eular.1271.
38. Luo XY, Liu Q, Yang H, et al. OSMR gene effect on the pathogenesis of chronic autoimmune Urticaria via the JAK/STAT3 pathway. *Mol Med*. 2018;24:28. https://doi:10.1186/s10020-018-0025-6.
39. Inoue G. Effect of interleukin-10 (IL-10) on experimental LPS-induced acute lung injury. *J Infect Chemother*. 2000;6:51–60. https://doi:10.1007/s101560000021.
40. van Rensburg IC, Wagman C, Stanley K, et al. Successful TB treatment induces B-cells expressing FASL and IL5RA mRNA. *Oncotarget*. 2017;8:2037–2043. https://doi:10.18632/oncotarget.12184.
41. Lee J, Dieckmann NMG, Edgar JR, et al. Fas Ligand localizes to intraluminal vesicles within NK cell cytolytic granules. *Immun. Inflamm Dis.* 2018;6: 312–321. https://doi:10.1002/iid3.219.
42. Barnett-Vanes A, Sharrock A, Eftaxiopoulou T, et al. CD43Lo classical monocytes participate in the cellular immune response to isolated primary blast lung injury. *J Trauma Acute Care Surg*. 2016;81:500–511. https://doi:10.1097/TA.0000000000001116.
43. Li J, Ding Y, Li A. Identification of COL1A1 and COL1A2 as candidate prognostic factors in gastric cancer. *World J Surg Oncol*. 2016;14:297. https://doi:10.1186/s12957-016-1056-5.
44. Kuivaniemi H, Tromp G. Type III collagen (COL3A1): gene and protein structure, tissue distribution, and associated diseases. *Gene*. 2019;707:151–171. https://doi:10.1016/j.gene.2019.05.003.
45. Astur DC, Novaretti JV, Cohen M. Genetic and molecular factors and anterior cruciate ligament injuries: current concepts. *Journal of ISAKOS: Joint Disorders & Orthopaedic Sports Medicine*. 2017;2:123–126. https://doi:10.1136/jisakos-2016-000115.
46. Aliseychik MP, Andreeva TV, Rogaev EI. Immunogenetic factors of neurodegenerative diseases: the role of HLA class II. *Biochemistry (Mosc)*. 2018;83: 1104–1116. https://doi:10.1134/S0006297918090122.
47. Huang PJ, Liu DZ, Gan XL, et al. Mast cells activation contribute to small intestinal ischemia reperfusion induced acute lung injury in rats. *Injury*. 2012;43: 1250–1256. https://doi:10.1016/j.injury.
48. Gan XL, Liu DZ, Huang PJ, et al. Mast-cell-releasing tryptase triggers acute lung injury induced by small intestinal ischemia–reperfusion by activating PAR-2 in rats. *Inflammation*. 2012;35:1144–1153. https://doi:10.1007/s10753-011-9422-5.